COMBINED HEATING AND COOLING NETWORKS WITH WASTE HEAT RECOVERY BASED ON ENERGY HUB CONCEPT

Hossein Ahmadisedigh, Louis Gosselin*

Department of Mechanical Engineering, Université Laval, Quebec City, Quebec, Canada

Article accepté pour publication dans : Applied Energy, Volume 253, November 2019

Abstract

Waste heat recovery can help reducing operation costs and greenhouse gas emissions. In the present work, an "energy hub" template was employed to design combined heating and cooling networks in which heat pumps can be used to recover heat from the cooling loop and supply it to the heating loop. Heating and cooling loads of the network can be satisfied by natural gas boilers, electric boilers, chillers, and heat pumps. The design of the system and its operation over the year were optimized with respect to cost and greenhouse gas emissions under different combinations of heating and cooling loads. The introduction of 8760-hour synthetic loads allowed covering several possible load profiles driving the energy hub. The contribution of each possible energy source and technology and the sizing of the heat pump system are optimized, while ensuring satisfaction of the heating and cooling demands. The optimized hub configurations for scenarios with and without waste heat recovery were compared, showing that heat pumps were beneficial in all scenarios. The optimal capacity of heat pumps to minimize total cost was found to be ~80% of the maximal possible value from a thermodynamic analysis of the loads. The simultaneous minimization of cost and emissions revealed a relatively sharp transition from gas to electric heating as more emphasis is put on emissions than cost, but in all cases, waste heat recovery with heat pumps was heavily used to satisfy the heating and cooling loads.

Keywords: heat pumps; energy hub; waste heat recovery; optimization; variable demand side

* Corresponding Authors: Louis.Gosselin@gmc.ulaval.ca; Tel.: +1-418-656-7829.

1. Introduction

Over the last years, the concept of "energy hub" has emerged as an appealing way to model complex energy conversion systems. The energy hub concept was introduced in Ref. [1], and the details of the corresponding project and its outcomes were discussed in [2], [3]. The energy hub concept models energy flows from various energy sources to different loads in an organized framework [4]. An energy hub contains three main components: (i) energy resources, (ii) energy convertors & storages, and (iii) energy demand (loads), and can be applied to a wide variety of systems.

Because of their flexibility, energy hub models are capable of handling various types of energy sources and carriers. Hence, depending on the energy sources that are available at the hub inlet, adapted equipment and technologies can be used to convert, transform or store energy. The energy sources can be fossil fuels, biomass, electricity from the grid or produced on-site, waste heat of a nearby plant, etc.

Since for a given set of electricity, heating, and cooling needs, there might be different combinations of energy sources to be used, it is important to determine which sources are more appropriate to satisfy the designated loads and which converters may offer the best performance. These various available energy sources can also cooperate in a synergetic way with other energy flows. For example, multi-generation facilities such as heat pumps or combined heat and power (CHP) systems are characterized by the fact that they can supply two different forms of useful energy at the same time. Heat pumps can provide simultaneous heating and cooling, whereas in CHP, both electricity and heat can be produced. These systems intrinsically provide a way to recover the waste heat from electricity or cold production. However, due to their complexity, a proper framework is required to model and optimize such energy systems, for example as that developed in the work of Geidl and Andersson [5]–[8].

The basic question in hub optimization is to determine at which rate each energy resource should be consumed by the system and at which rate each converter should contribute in supplying the loads (i.e., operational optimization). Furthermore, one may be interested in optimizing the hub configuration itself and the choice of technologies on which it relies (i.e., design optimization). These optimization problems can be formulated and analyzed using various criteria such as cost, GHG emissions, etc.

In operational optimization of energy hubs, studies focus on finding the optimal contributions of each energy carrier in order to satisfy the end-user demands. In this line,

Schulze, Friedrich and Gautschi [9] presented an application of energy hub as a modeling framework for optimal power flow problems with integrated energy systems and multiple energy carriers. They modeled an energy hub within a single time step with constant efficiencies and illustrated the application of the model with a realistic hub comprising five different energy sources.

A dual-objective optimization aiming to minimize both cost and GHG emissions with the weighted-average sum method is presented by Maroufmashat, Elkamel, Fowler et al. [10]. They used the optimization tool General Algebraic Modeling System (GAMS) to solve a Mixed-Integer Linear Problem (MILP) with the CPLEX solver. Each part of the objective function (i.e., cost and GHG emissions) is normalized by its minimum value when it is regarded as the only objective function. A comprehensive study of normalization methods for the weighted average sum approach is discussed in [11].

The optimization problem proposed by Moghaddam, Saniei and Mashhour [12] includes a detailed model of a residential energy hub designed to meet the heating, cooling, and electrical needs of a building. The possibility to sell electricity to the grid is also considered. The analysis of the daily scheduling of the energy hub is performed in GAMS as a Mixed-Integer Non-Linear Program (MINLP). On the contrary, a MILP formulation is employed in [13], in which the possibility of using different combinations of energy converter and storage devices is assessed. The approach taken in the latter involves a comprehensive model for planning the energy hub configuration.

To adapt energy hubs to interconnected regions with different energy resources and policies, the concept of Regional Energy Hub is developed by Guler, Çelebi and Nathwani [14]. In this approach, each participating region can get benefits from the mutual advantages of a shared hub. Reducing carbon emissions and costs are the major targets. From the recent work presenting more complex and comprehensive methods to model energy hubs, the research by Ayele, Haurant, Laumert and Lacarrière [15] can be mentioned here. Their model analyzes complex couplings of local heating and electricity networks. The couplings are modeled within an energy hub framework using Matlab.

A network of four interconnected energy hubs is optimized from the cost standpoint by Maroufmashat, Fowler, Sattari Khavas et al. [16]. The capital cost of hydrogen refueling stations and operation cost of energy hubs were taken into account. The associated MILP is solved with the CPLEX solver for 8,760 hours (i.e., 1 year). The study calculates the optimal

operation of various pieces of equipment for energy conversion and storage in order to satisfy the demand for a single objective (i.e., cost) problem.

In some studies, authors begin with a set of predefined possible scenarios for the system configuration and compare these configurations. In [17], the authors used Mixed Complimentary Problem (MCP) in GAMS to deal with an economic model. They developed different scenarios that combine different energy generation technologies and evaluate generated energy, cost, and emissions. A similar approach was adopted in [18]. They regarded emissions as an element in the cost function of their MCP to find the best operational and design criteria among the available scenarios. In both aforementioned papers, all efficiencies are held constant over the year, and a time step of 1 h is used which requires 8,760 time steps to simulate 1 year. Togawa, Fujita, Dong, Fujii and Ooba [19] studied the replacement of a boiler with different scenarios to meet the heating demand of a greenhouse.

Reliability and uncertainty of energy hubs are assessed in [20] and [21], respectively. In [20], reliability is imposed as a constraint during the modeling phase, compared to [21], in which cost and emissions are minimized as objective functions. The optimization operates under uncertainty of electricity price, electricity demand, and wind power in different scenarios. Both above-mentioned articles have optimized their models with a CPLEX solver. All capital costs entered as presumed constant values in the cost analysis and optimization procedures.

In the work done by Brahman, Honarmand and Jadid [22], Demand Response (DR) and energy storage are highlighted, and single and multi-objective optimization are performed for a 24-hour time period with mixed-integer linear programming (MILP) via the CPLEX solver. A similar research by Batić, Tomašević, Beccuti, Demiray, and Vraneš [23] also focuses on Demand Side Management (DSM) with a time step of 15 minutes during a special day of the year. Heating loads are estimated using Matlab and the single objective optimization is performed by CPLEX. Energy Management System using Dynamic Pricing (DP) and Time-of-Use methods is investigated in Ref. [24] thorough an energy hub concept. A 24-hour time step is used for time series input and output. Operational cost of fuel, water, and electricity, as well as discomfort costs (due to load shifting) is the objective function. Efficiencies are constant and the model is linear.

So far, only 8% of the articles related to energy hubs have employed heat pump technology in their hub modeling and/or optimization [25]. In Refs. [12] and [13], the possibility of using an electric heat pump, a CHP, and an absorption chiller (all three can work

as waste heat recovery (WHR) modules) within an energy hub is analyzed. In the former, the implementation of the WHR component is discussed at a residential scale, whereas in the latter, it models an overall energy hub is assumed without any predetermined configuration for the hub. The hub comprising energy converters and storages is optimized from operational and structural points of view with respect to the total cost.

In Refs. [26]–[28], the inclusion of Combined Heating and Power (CHP) and Combined Cooling, Heating and Power (CCHP) in the energy hub are assessed. Optimal operational and configuration characteristics of a hub including CHP units are addressed in a MILP by Moradi, Ghaffarpour, Ranjbar and Mozaffari [26], with respect to supply reliability. In [27], [28], the optimization of an energy hub, with a focus on Combined Cooling, Heating and Power (CCHP) systems, is studied. A single objective optimization is used based on cost to find the optimum size of hub elements such as gas turbine, heat exchanger, absorption chiller, boiler, storage system and electricity transformer. GHG emissions are accounted for as an imposed cost on the system. GAMS and COMFAR are used to solve the associated non-linear problem. All efficiencies are assumed constant in their modeling.

Through the above literature review, several limitations and gaps were identified and will be addressed in the present work. Thermal integration of heating and cooling networks through the hub concept has not received a lot of attention, even though these energy systems are among the most common, ranging from small systems in individual buildings to more elaborate ones in districts and plants. Developing a better understanding of how and when waste heat recovery can be integrated in heating and cooling networks is thus required and could be quite impactful in terms of energy conservation. Furthermore, the impact of the heating, cooling and electric loads on the features of the optimal hub design and operation is typically not investigated, as only one or a few load profiles are used in a given study. It would thus be useful to evaluate this impact of the load on the optimal design and provide designers with general charts of the best designs as a function of the load context.

In this paper, we introduce a hub model to optimize the operation and design of a combined cooling and heating network. In particular, waste heat recovery opportunities with the use of heat pumps through the integration of these networks are studied. In Section 2, the energy hub model is introduced, along with the formulation of the optimization problem. The solver is presented in Section 3. Section 4 presents the resulting design and operation of the combined heating and cooling network when minimizing total cost, and Section 5 introduces correlations to easily size the system based on the parameters of the problems. Finally, a dual-

objective problem (minimizing simultaneously cost and GHG emissions) is introduced and solved in Section 6. The paper aims at facilitating the design and implementation of waste heat recovery strategies such as the integration of heat pumps in a combined heating and cooling network. It provides a detailed design methodology, as well as new design charts and correlations for easily pre-sizing the system in practice.

2. Energy hub optimization model

2.1 Modeling of the system

The energy system that is studied in this paper is schematized in Fig. 1 in the form of an energy hub. It consists in a heating and cooling system, which was initially inspired by the district heating and cooling network of the campus of Université Laval (Québec City, Canada). Chillers (labeled "ch" in Fig. 1) produce chilled water that circulates in a loop from which buildings are cooled. The heat extracted from the buildings is delivered to the cold loop, and is eventually rejected to the ambient in cooling towers that are connected to the chillers, and thus becomes waste heat. Heating is provided to the buildings by a vapor or a hot water network which constitutes a second loop. Two types of boilers are considered depending on the source of energy (i.e., electricity and natural gas, respectively "eb" and "fb" in Fig. 1). Once heat is taken from the vapor/hot water, the condensate/water is returned to the boilers. In general, these two loops (e.g., chilled water and vapor/hot water) are considered independent. In this paper, we assume that the system (without heat pumps) already exists and we investigate the potential to recover heat from the cold loop with new heat pumps in order to supply heat to the buildings and produce chilled water at the same time. Note that because of the temperatures involved in this type of system are close to the ambient, the actual exergy of the waste heat is quite low, even though the amount of energy available can be significant. This emphasizes the recourse to a direct use of the waste heat as proposed here, rather then using it to produce electricity.

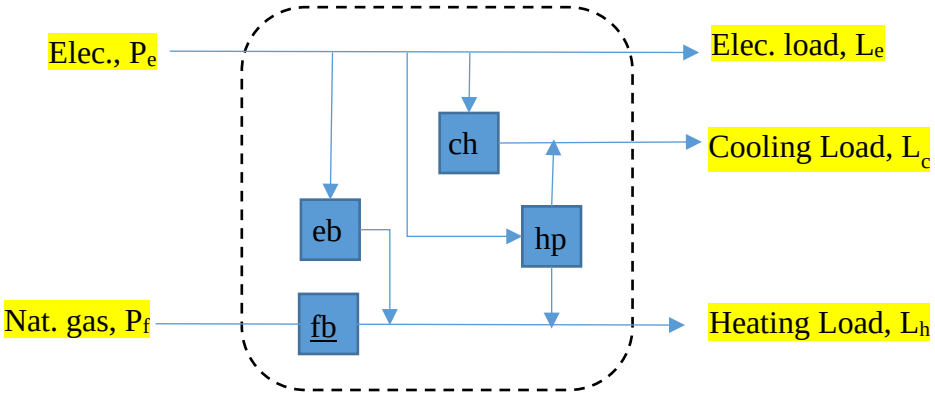

Figure 1: Hub representation of a heating and cooling network including electrical and natural gas boilers (eb and fb), chillers (ch) and heat pumps (hp).

Because there is no local electricity generator or power plant in the system considered, the electricity demand should be met directly by the grid. In the present model, the electricity demand was separated into four parts: the electricity required by the chiller, by the heat pumps, by the electric boiler and the remaining electricity demand (which is labeled L_e in Fig. 1). In this way, it is possible to assess how changes to the design or operation of the hub affect the electricity cost, which is also a function of the monthly peak demands as will be shown below. As can be seen in Fig. 1, the cooling load L_c is satisfied by the chillers and heat pumps, and the heating load L_h, by the heat pumps and the two types of boilers. The different loads identified in Fig. 1 (i.e., L_e, L_h and L_c) pull energy fluxes from the two available sources, i.e. from the electric grid (i.e., P_e) and from natural gas (i.e., P_f). Note that since L_e, L_h and L_c vary in time, so do P_e and P_f.

The general equation of an energy hub relates the energy resource vector **P** and the load vector **L**, and can be expressed by

$$\underbrace{\begin{pmatrix} L_e \\ L_c \\ L_h \end{pmatrix}}_{\mathbf{L}(t)} = \underbrace{\begin{pmatrix} C_{ee} & C_{fe} \\ C_{ec} & C_{fc} \\ C_{eh} & C_{fh} \end{pmatrix}}_{\mathbf{C}} \underbrace{\begin{pmatrix} P_e \\ P_f \end{pmatrix}}_{\mathbf{P}(t)} \tag{1}$$

where **C** is the coupling matrix and includes all the conversion and transformation coefficients corresponding to the hub technologies. *P* denotes the power of each energy resource that has been shown by *f*, *e* representing fuel (natural gas), and electricity, respectively. The subscripts c, h also indicate cold and heat on the demand side. This way, the subscript *fe*, for instance, means the conversion factor for fuel (natural gas) to electricity.

In the present case, the coefficients C_{fe} and C_{fc} are equal to zero, since the fuel is not used to satisfy the electric load, nor the cooling load. The C-coefficients involve the share of the energy resources that are used by the different end-uses, and the efficiency of the different technologies. Again, it should be reminded that Eq. (1) must hold true at each time step.

In the present model, it was decided to rewrite the hub model by splitting the total electricity consumed from the grid, P_e, as the summation of the different contributions mentioned above, i.e. electric heaters ($P_{e,EH}$), heat pumps ($P_{e,HP}$), chillers ($P_{e,CH}$), and other end-uses (L_e):

$$P_e = P_{e,EH} + P_{e,HP} + P_{e,CH} + L_e \tag{2}$$

Note that the share of the electricity used for the other end-uses was written as L_e since this correspond to the electric load in the present problem (see Fig. 1). An equivalent form to Eq. (1) is obtained by expressing the heating and cooling loads as a function of these different electricity consumptions and of the fuel consumption:

$$L_h = \eta_{fh}^{B} P_f + \eta_{eh}^{B} P_{e,EH} + \eta_{eh}^{HP} P_{e,HP} \tag{3}$$

$$L_c = \eta_{ec}^{CH} P_{e,CH} + \left(\eta_{eh}^{HP} - 1\right) P_{e,HP} \tag{4}$$

Note that HP, B, CH, EH, h, c, ec, and eh denote heat pump, natural gas boiler, chiller, electric heater, heat, cold, electricity to cold and electricity to heat, respectively. The η -values are the efficiency of each energy convertor. In the present study, these efficiency values are kept constant ($\eta_{fh}^{B} = 0.85$, $\eta_{eh}^{HP} = 6$, $\eta_{eh}^{CH} = 4$, $\eta_{eh}^{EH} = 0.95$), but future work could include a dependency on time, part-load ratios, temperature, etc. Note that η_{eh}^{HP} can be seen as the coefficient of performance of the heat pump based on heating mode, whereas $\eta_{eh}^{HP} - 1$ is the coefficient of performance of the heat pump based on cooling mode (COP_c). Typical values of COP_c vary between 3 to 5 for water-to-water heat pumps [29]. It should be noted that advanced heat pumps are considered in the present study, with large COP values and with variable speed drive. This features allows to modulate the load that is "taken in charge" by the heat pump as seen in Eqs. (3)-(4). Having several different heat pumps would also be a way to help modulating their load. If one single speed heat pump would have been used (e.g., see Setlhaolo, Sichilalu and Zhang [30]), on/off decision variables for the heat pump could be introduced in the problem instead of optimizing the load to the heat pump system.

In a matrix form, the energy balance of Eqs. (3)-(4) becomes:

$$\begin{pmatrix} L_c \\ L_h \end{pmatrix} = \begin{pmatrix} \eta_{ec}^{CH} & \left(\eta_{eh}^{HP} - 1\right) & 0 & 0 \\ 0 & \eta_{eh}^{HP} & \eta_{eh}^{EH} & \eta_{fh}^{B} \end{pmatrix} \begin{pmatrix} P_{e,CH} \\ P_{e,HP} \\ P_{e,EH} \\ P_f \end{pmatrix} \tag{5}$$

This model will be used to represent the behavior of the hub. The loads L_c, L_h and L_e are assumed to be known at all time steps, as well as the different efficiencies of the convertors. The problem consists in finding the optimal vector **P** at all time steps (i.e. to what extent each technology should be used to supply heat and cold). The hub model of Eq. (5) will serve as an equality constraint in the optimization process that will be described below.

In order for the hub model to be physically sound, it is necessary to invoke other constraints. First, all P-values must always be larger or equal to zero at each time step, i.e.:

$$\begin{pmatrix} P_{e,CH} \\ P_{e,HP} \\ P_{e,EH} \\ P_f \end{pmatrix} \geq 0 \tag{6}$$

Furthermore, the different convertors have a limited capacity due to the sizing of each piece of equipment, which translates as:

$$\begin{aligned} \eta_{ec}^{CH} P_{e,CH} &\leq Q_{CH,\max} \\ \left(\eta_{ec}^{HP} - 1\right) P_{e,HP} &\leq Q_{HP,\max} \\ \eta_{eh}^{EH} P_{e,EH} &\leq Q_{EH,\max} \\ \eta_{fh}^{B} P_f &\leq Q_{B,\max} \end{aligned} \tag{7}$$

In this series of inequalities, $Q_{CH,max}$ is the maximal capacity of the chillers, $Q_{HP,max}$, the maximal cooling capacity of the heat pumps, $Q_{EH,max}$, the maximal capacity of the electric heaters, and $Q_{B,max,}$ the maximal capacity of the natural gas boilers. In the present problem, we assumed that $Q_{CH,max}$ and $Q_{B,max}$ were known and fixed. They would correspond to the current system (i.e. they are already in place) and their value should be large enough to satisfy the different loads. For the sake of simplicity, it was assumed that $Q_{CH,max} \rightarrow \infty$ and $Q_{B,max} \rightarrow \infty$. Similarly, the size of the electric heater ($Q_{EH,max}$) was known and fixed, and in this study it assumed a value of 5,133 kW (i.e., 20,000 lbm/h).

Finally, the size of the heat pump system, $Q_{HP,max}$, was considered as a decision variable. In other words, one wants to find whether it is profitable to purchase heat pumps and determine what capacity is needed. In order to obtain only non-negative values, the following constraint needs to be invoked:

$$Q_{HP,\max} \geq 0 \tag{8}$$

2.2 Objective functions and optimization problem

The first objective function is the total cost, including annual operation cost C_{op} and the purchase cost C_{init}^{HP}:

$$C_{tot} = C_{init}^{HP} + \frac{(1+i)^n - 1}{i(1+i)^n} C_{op} \tag{9}$$

where i is the interest rate, and n the duration of the project. In the present work, we used i = 5% and n = 10 years. Since the present study is focused on the addition of heat pumps to an existing system, only the purchase cost of the heat pumps is considered in the initial costs. In other words, it is assumed that all other pieces of equipment are already in place and thus, do not need to be purchased. If a new system were to be designed from scratch, the cost of the other pieces of equipment (e.g., boilers, chiller, etc.) would need to be included. The unit price of heat pump is estimated based on the correlation introduced in [29], in such a way that:

$$C_{init}^{HP} = \phi_{HP} Q_{HP,\max} \tag{10}$$

with ϕ_{HP} = 230 CAD/kW.

The annual operation cost is related to the energy consumption of fuel and electricity,

$$C_{op} = C_{op,e} + C_{op,f} \tag{11}$$

where the cost associated to the fuel consumption is simply the amount of fuel consumed multiplied by the unit cost of fuel:

$$C_{op,f} = \phi_f \sum_{t=1}^{N} P_f(t) \Delta t \tag{12}$$

with the unit cost of fuel ϕ_f equal to 0.15 CAD/m^3 (0.016123 CAD/kWh) [31]. The cost of electricity includes two components, i.e. the cost for the amount of energy consumed and the cost for the monthly peak demand:

$$C_{op,e} = \phi_{e,energy} \sum_{t=1}^{N} P_e(t)\Delta t + \phi_{e,peak} \sum_{month=1}^{12} \max\left(P_e(t)\right) \quad (13)$$

where the unit costs $\phi_{e,energy}$ and $\phi_{e,peak}$ are respectively 0.0327 CAD/kWh and 12.87 CAD/kW, based on current price for large consumers in Quebec, Canada [32]. Note that the first summation is over all the time steps, and the second summation is over the different months since peak demands are charged on a monthly basis.

A second objective function was also studied, namely the greenhouse gases emissions (GHG) in $CO_{2,eq}$ associated with a solution. The total annual energy-related emissions are:

$$CO_{2,tot} = CO_{2,e} + CO_{2,f} \quad (14)$$

where:

$$CO_{2,e} = \lambda_e \sum_{t=1}^{N} P_e(t)\Delta t \quad (15)$$

$$CO_{2,f} = \lambda_f \sum_{t=1}^{N} P_f(t)\Delta t \quad (16)$$

The emission intensities of electricity and fuel were respectively λ_e = 0.02072 kg $CO_{2,eq}$/kWh [33] and λ_f = 0.17644 kg $CO_{2,eq}$/kWh [34] for Quebec, Canada. Note that the GHG emissions related to electricity are very low because electricity in Quebec is almost entirely hydroelectricity.

3. Optimization solvers

The optimization problem introduced in Section 2 can be formulated as: minimize C_{tot} (Eq. (9)) and/or $CO_{2,tot}$ (Eq. (14)) with respect to the 4N+1 decision variables (i.e., $Q_{HP,\max}$, $P_{e,CH}(t)$, $P_{e,HP}(t)$, $P_{e,EH}(t)$, $P_f(t)$), while respecting 2N equality (Eq. (5)) and 8N+1 inequality constraints (Eqs. (6)-(8)), where N is the number of time steps. With a one-hour time step, one has N = 8,760 in order to simulate one year of operation. In that case, the number of decision variables is 35,041 and the number of constraints is 87,601. Furthermore, the optimization problem introduced above is non-linear due to the peak of electricity demand, max(P_e), which appears in the cost evaluation . Different solvers were considered to solve the problem. Although some non-linear solvers provided satisfying optimization results (e.g., SCIP, LINDO), the computational time was important. It was thus decided to linearize the problem.

The maximum function in Eq. (13) can be converted into a mixed-integer linear problem using a binary variable *K(t)* [35]. This variable will be zero in every time slot except that with the maximum electricity demand for which $K = 1$. Therefore, $\max(P_e)$ in Eq. (13) is replaced by $P_{e,peak}$ (which becomes a new decision variables in the linearized problem), given that the following constraints are respected:

$$P_{e,peak} \geq P_e(t) \tag{17}$$

$$P_{e,peak} \leq P_e(t) + M\left(1 - K(t)\right) \tag{18}$$

$$\sum_t K(t) = 1 \tag{19}$$

where M is a large number that must be chosen so that it is larger than the difference between the maximum and minimum values of $P_e(t)$. Eq. (17) ensures that $P_{e,peak}$ is large enough to be above or equal to $P_e(t)$. In Eq. (18), when K=1 at a given time step (i.e. when the peak occurs at that time step), the inequality forces $P_{e,peak}$ to be limited by the actual value of $P_e(t)$. In our case, since 12 peak months must be taken into account, there are 12 $P_{e,peak}$ variables (one per month), and Eqs. (17)-(19) are treated on a monthly basis. The linearization introduces N binary variables, 12 continuous variables, and 2N inequality constraints.

Different MILP solvers were tested. In the end, the CPLEX solver was chosen. The computational time for one optimization run is approximately 40 s.

The model was carefully tested to ensure that it contained no errors. For example, a scenario with no cooling load was modeled. It was verified that chillers were not used and that heat pumps were not present in the design. Similarly, when no heating is present, it was verified that heat pumps, boilers and electric boiler did not contribute in the network. In the limit where the purchase cost of heat pumps tends to infinity, heat pumps are not employed, and thus, chiller is generating the entire needed cold; also, the heating load is totally fed by electric and natural gas boilers. In the limit where the peak cost was increased to large values, the usage of electricity in all devices tend to fall by using as much fuel as possible in boilers, and the cooling load is met solely by the heat pump.

4. Analysis of cost-minimal systems under different load scenarios

In the optimization problem introduced above, loads need to be provided. For the sake of simplicity, the following synthetic load functions were used in the present work:

$$L_x = A_{x,a} + A_{x,y} \sin\left(2\pi \frac{t}{\tau_y} + \theta_{y,x}\right) \tag{20}$$

where "x" can be either "h" or "c", depending on whether heating or cooling loads is considered. τ_y is the duration of a year. In the end, each load is characterized by 3 parameters (i.e., $A_{x,a}$, $A_{x,y}$, and $\theta_{y,x}$). This synthetic load representation was chosen for its simplicity and its capacity to represent realistic loads.

Although the synthetic load of Eq. (20) is only a simulated profile of the heating and cooling demands, it provides the optimization model with a realistic approximation of typically encountered situations (e.g., maximum cooling load during summer and minimum cooling in the winter, and vice versa for the heating load). Even though differences between real-case profiles and the synthetic curves could lead to different optimal design and operational solutions for the system, the methodology proposed here to optimize the system can still be applied.

In the present work, we assumed that the cooling load L_c was zero in the beginning of the year, reaching its maximal value in the middle of the year (i.e. $\theta_{c,y} = -\pi/2$) with an amplitude $A_{c,y}$ varying from 0 to 50 MW. The heating load was defined similarly, except that the maximum occurred in the beginning/end of the year and that a zero load was found in the middle of the year (i.e., $\theta_{c,y} = \pi/2$) with an amplitude $A_{h,y}$ between 0 and 50 MW. An important feature of this problem is that the solution to the cost minimization problem is not influenced by L_e in this case. It should be remembered that the electricity load L_e is the total electricity load minus the electricity used for heating and cooling, and that the electricity share of the pieces of equipment that are used for heating and cooling (i.e., heat pump, chiller and electric heater) is calculated separately, as described above, Eqs. (5) and (13). Thus, optimal heat pump size and GHG emissions depend only on heating and cooling demands. The electric load L_e itself represents a certain cost, calculated within Eq. (13). As the optimization takes place, some components consume more or less electricity (electric boiler, chiller, heat pumps) which induces an additional cost for electricity. However, this additional cost is independent from the baseline cost for L_e. Therefore, performing the cost minimization for different combinations of heating and cooling loads (i.e., for several sets of $A_{h,y}$ and $A_{c,y}$) is sufficient to fully characterize the optimal system as a function of the load. The load profiles are summarized in Fig. 2.

The cooling and heating load amplitudes were varied independently between 0 and 50 MW, by 10 MW increments, and in each case, the system was optimized by the procedure described above. In the present section, only the total cost is considered as the objective function (one objective). It should be noted that cost-minimal designs are of particular interest in practice. It is traditionally what practice engineers try to achieve. This justifies the relevance of the present section which presents resulting optimal design as a function of load scenarios. Simultaneous minimization of cost and GHG emissions will be treated subsequently. All possible combinations of $A_{h,y}$ and $A_{c,y}$ were simulated, for a total of 36 optimization runs. The resulting optimal systems (i.e., cost minimal system) were then compared to the reference systems, which correspond to the energy hub without heat pumps.

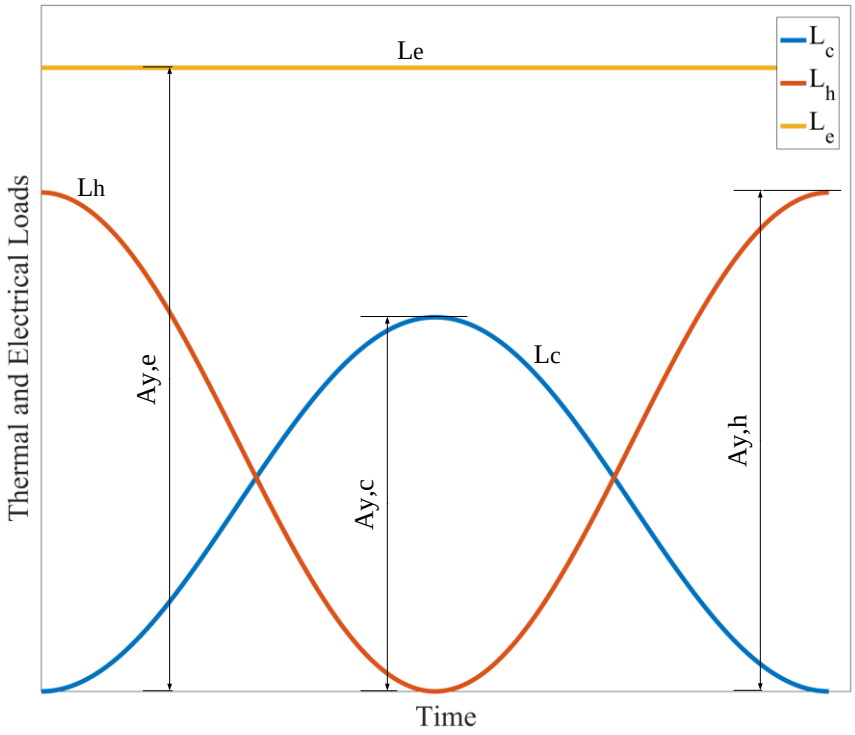

Figure 2:Schematic representation of the heating, cooling and electricity loads

Figure 3 reports the energy savings ΔC achieved by introducing heat pumps into the hub compared to the reference case, i.e. the reference cost minus the minimized total cost of the hub with heat pumps.. This figure is based on minimizing the total cost of the system. A positive value of ΔC means that savings are achieved with heat pumps, whereas zero or negative ΔC values would imply that the project is not profitable. It is visible in Fig. 3 that the integration of heat pumps becomes more and more beneficial as the thermal loads are increased, and in particular when they both increase simultaneously.

Figure 4 shows the optimized size of the heat pump as a function of the thermal loads. As expected, the higher the heating and cooling loads, the bigger the optimal capacity (size) of the heat pump. Note that the yellow points in Fig. 4 correspond to specific load scenarios that will be analyzed below. It should be remembered that Figs. 3-4 were obtained by minimizing the total cost only. As mentioned above, cost is often the driving objective in this type of project. In that case, Figs. 3-4 can be seen as practical design charts for sizing heat pumps in synergetic heating and cooling networks, and estimating the potential annual savings.

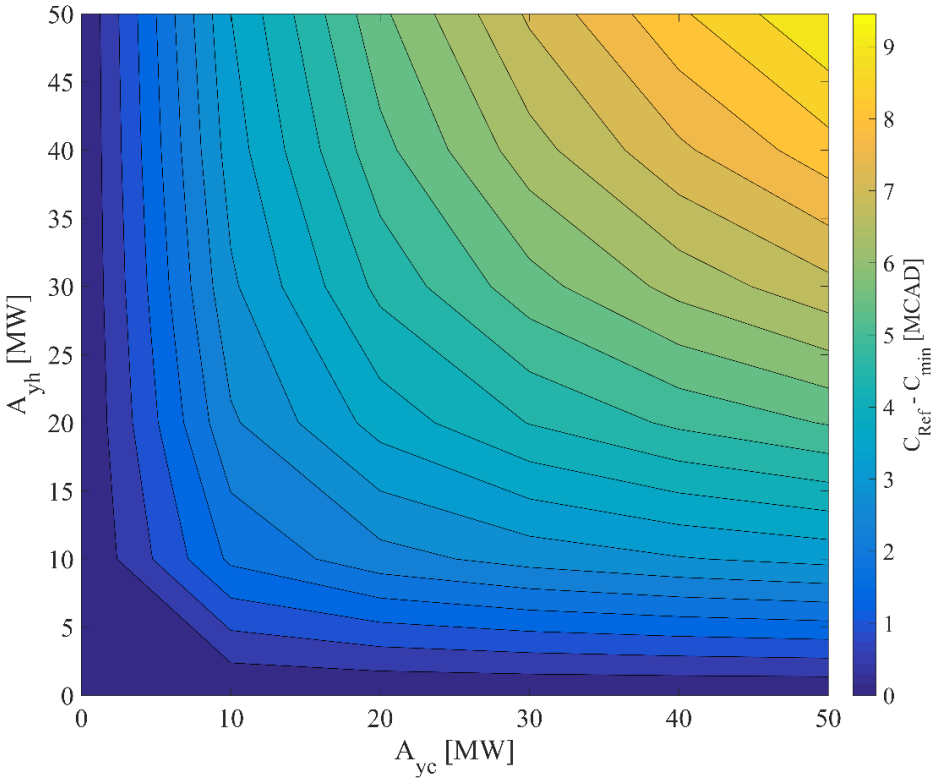

Figure 3:Savings caused by heat pumps (cost difference between the reference hub and that cost-minimized hub with the heat pumps) as a function of the heating and cooling

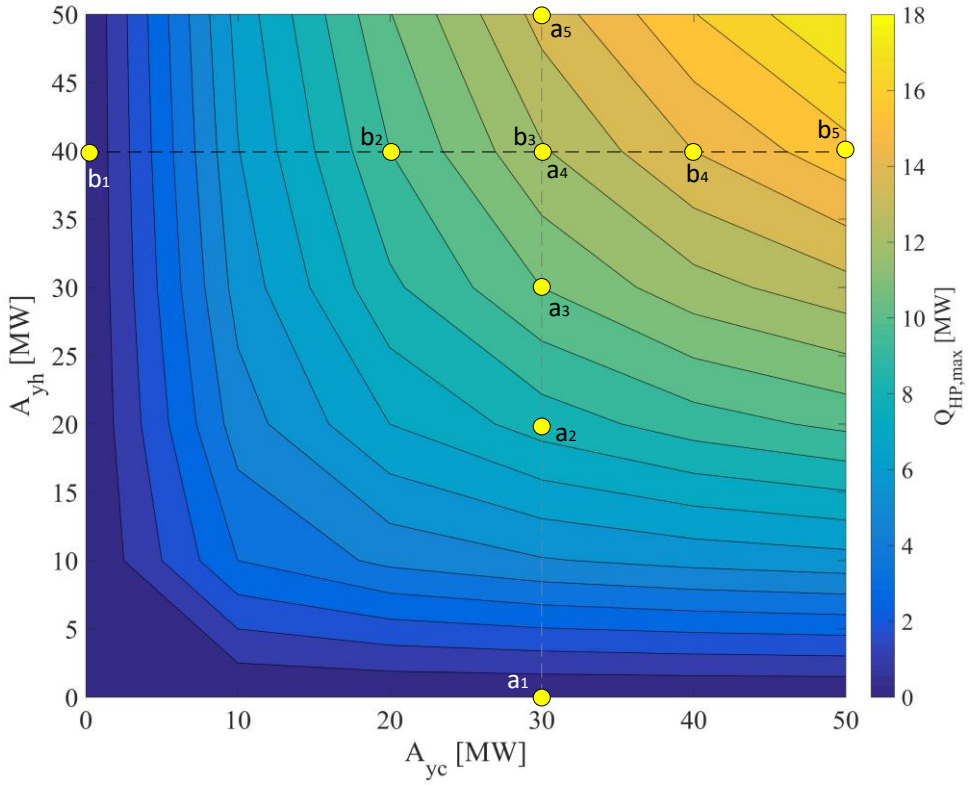

Figure 4:Optimal heat pump capacity as a function of the heating and cooling loads with constant electrical load.

5. Scale analysis to explain cost-minimal results

A scale analysis is developed in the present section. As will be shown below, this approach helps developing a better understanding of the features of cost-minimal systems both in terms of their design (i.e., size of the heat pump) and operation (i.e., how the heat pump is used). Furthermore, simple expressions will be obtained from this analysis to predict the optimal size of heat pumps integrated in an existing cooling and heating network. These expressions could be used in practice at the pre-design stage of a project.

The analysis starts by realizing that in the optimized hub, the consumption of electricity by the heat pump must always be smaller than the following limit:

$$P_{e,HP}(t) \leq \min\left\{\frac{L_c(t)}{\eta_{eh}^{HP}-1}, \frac{L_h(t)}{\eta_{eh}^{HP}}\right\} \tag{21}$$

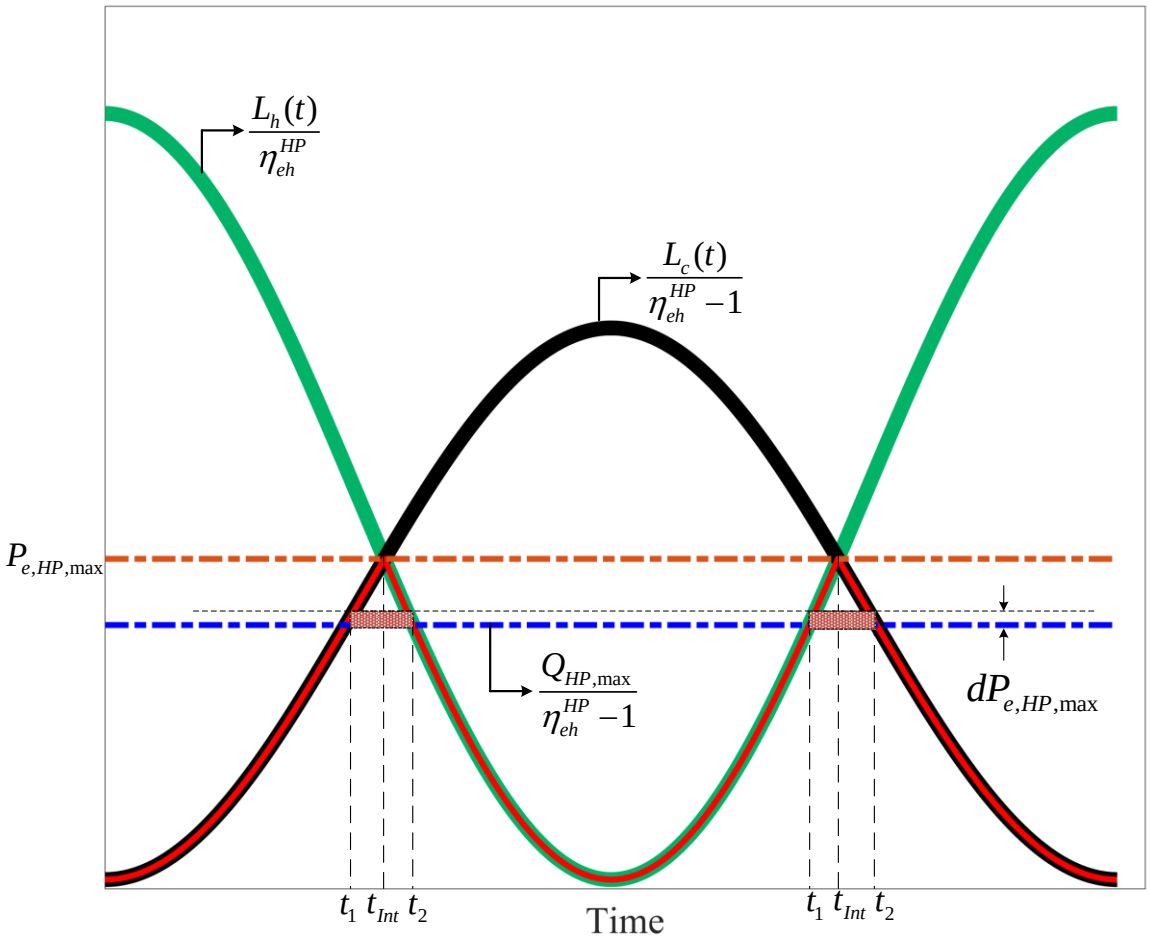

Figure 5: Schematic representation of the ceiling value of the heat pump electricity consumption

The first term in the accolade is the heat pump electricity load that would be obtained if the entire thermal cooling load of the system served by the hub was to be satisfied by the heat pump. Equivalently, the second term is the electricity required at the heat pump in order to satisfy entirely the heating load. In the end, whichever of these two terms is smaller provides a maximal ceiling value of what the heat pump could provide at a given time step. In other words, during the optimization, it is not useful for the heat pump to provide more heating or cooling than that dictated by the smallest loads. For the sake of illustration, $L_c(t)/\eta_{eh}^{HP}-1$ and $L_h(t)/\eta_{eh}^{HP}$ are plotted in Fig. 5. The right-hand side of Eq. (21) is also shown by the red envelope in Fig. 5 and defines the maximal possible value of $P_{e,HP}(t)$ at each time.

Moreover, the peak of the red envelope in Fig. 5 provides a ceiling value for the heat pump sizing. In other words, it would make no sense for the optimized heat pump capacity to be such that it would require more electricity than that peak. It is possible to obtain an analytical

expression for this peak, first by intersecting the "reduced" loads, i.e. by setting the expression $L_c(t)/\eta_{eh}^{HP} - 1 = L_h(t)/\eta_{eh}^{HP}$, which yields the time at which the intersect occurs (see Fig. 5):

$$t_{Int} = \frac{\tau_y}{2\pi} \text{Arc}\cos\left(\frac{A_c\,\eta_{eh}^{HP} - A_h(\eta_{eh}^{HP} - 1)}{A_c\,\eta_{eh}^{HP} + A_h(\eta_{eh}^{HP} - 1)} \right) \tag{22}$$

Then, the reduced load at this time is calculated, and one finds that the peak of the envelope in Fig. 5 is:

$$P_{e,HP,\max} = \frac{A_{h,y} A_{c,y}}{A_c\,\eta_{eh}^{HP} + A_h(\eta_{eh}^{HP} - 1)} \tag{23}$$

The optimized heat pump electricity consumption over time was then compared and normalized with respect to the envelope curve (in red) of Fig. 5 and to the peak of that envelope (Eq. (23)):

$$P_{e,HP,Norm}(t) = \frac{P_{e,HP}(t)}{P_{e,HP,\max}} \tag{24}$$

To have a better understanding of how heat pump contributes to the generation of heating and cooling in the system, heat pump normalized electricity usage $P_{HP,Norm}$ (see Eq. (24)) is shown in Fig. 6 as a function of time, as well as cooling and heating load amplitudes. Results from the optimization runs performed in the previous section were used. For the sake of visibility, from the 36 above-mentioned load combinations, only 9 cases with different cooling and heating amplitudes were chosen to illustrate the heat pump electricity consumption over time. On the left hand side of Fig. 6, the cooling load amplitude $A_{c,y}$ is 30 MW while the heating load amplitudes vary between 0 and 50 MW. These curves corresponds to points a_1-a_5 in Fig. 4. Similarly, the right hand side of Fig. 6 represents the consumption of the heat pump with $A_{h,y}$ = 40 MW and $A_{c,y}$ between 0 and 50 MW, i.e. for points b_1-b_5 in Fig. 4. In this figure, we took advantage of the symmetry of each profile at mid-year to represent only half of each curve.

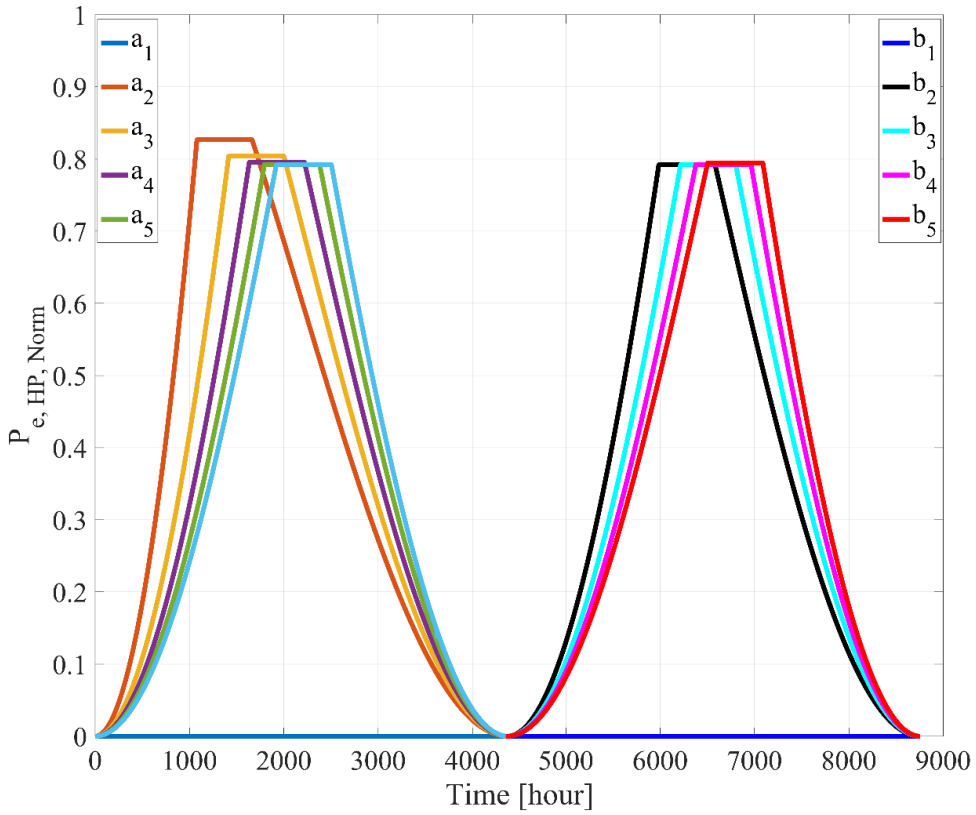

Figure 6: Normalized heat pump electricity consumption versus time for 9 load scenarios corresponding to the yellow points in Fig. 4

As apparent in Fig. 6, the actual curves tend to follow the conceptual red envelope of Fig. 5, but also exhibit a flat portion during which heat pumps generate a constant amount of heat. On this plateau, the heat pump is used at full capacity and the extra heat required is supplied by boilers. The ratio of the maximum optimal heat pump electricity consumption to the maximum theoretical electricity usage of heat pump is defined as:

$$k = \frac{P_{e,HP,\max\,opt}}{P_{e,HP,\max}} = \frac{\left(A_c\,\eta_{eh}^{HP} + A_h(\eta_{eh}^{HP} - 1)\right) P_{e,HP,\max\,opt}}{A_{h,y} A_{c,y}} \tag{25}$$

In other words, the value of k corresponds to the value at which the plateau occurs in Fig. 6, i.e. the percentage of the maximal thermodynamic limit for the heat pump capacity based on the heating and cooling loads that should be installed. In Eq. (25), $P_{e,HP,max,opt}$ denotes the maximum electricity usage of the heat pump as a consequence of the optimization process. The value of k was found to be almost insensitive to the load scenario and varies only between 0.79 to 0.83 (see the plateaus in Fig. 6).

Based on the observation that there is an optimal value of k which is almost the same for all load cases, there is thus an opportunity to try predicting the heat pump optimal capacity (by multiplying $P_{e,HP,max,opt}$ (η_{HP}-*1*)), even prior to optimization. In Fig. 7, the optimized heat pump

capacity was plotted against the thermodynamic ceiling value, Eq. (23), for all the load scenarios. Each point is the result of a full optimization as explained in the previous sections. A linear fitting was then applied and is also shown in Fig. 7. The slope of the linear fitting actually corresponds to the value of k that best-fits all the results (k = 0.7961). In other words, it is possible to predict the optimal capacity of the heat pump to be purchased with the following correlation:

$$Q_{HP,\max,\mathrm{Est}} \approx 0.7961 \underbrace{P_{e,HP,\max}\left(\eta_{eh}^{HP}-1\right)}_{Eq.(23)} \tag{26}$$

where $Q_{HP,max,Est}$ represents the estimated optimal size of the heat pumps to be provided in the system.

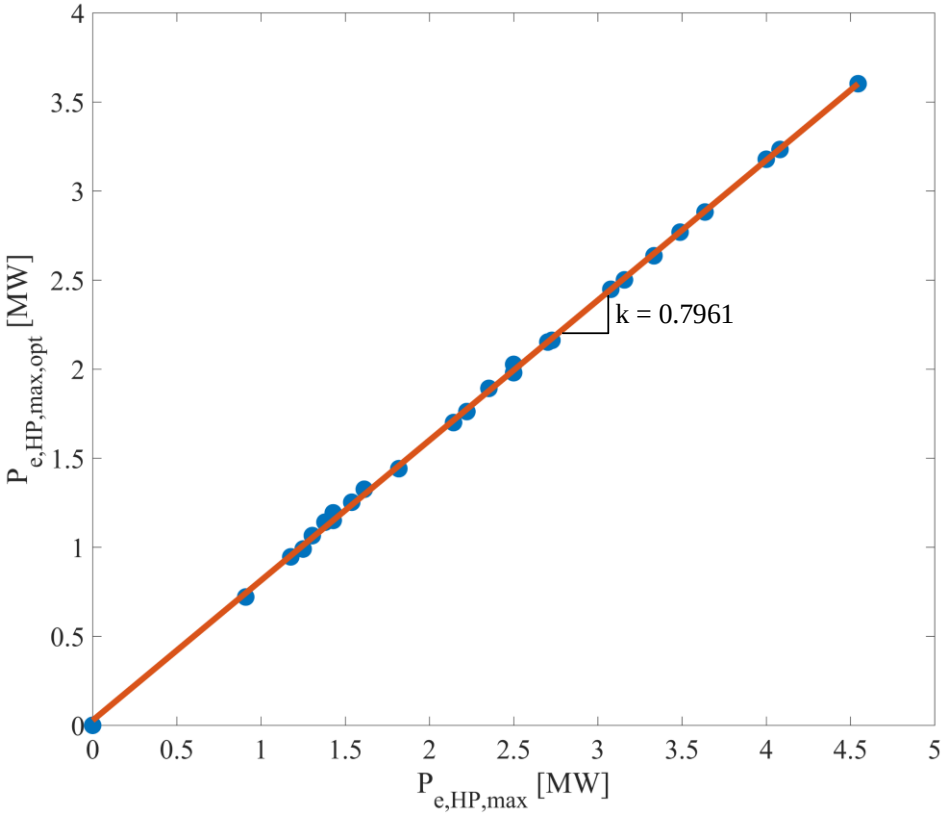

Figure 7:Optimized peak heat pump electricity consumption versus thermodynamic limit based on loads

The value of k = 0.7961 means that the optimal heat pump capacity is about 80% of the theoretical maximum heat pump size based on the load analysis (i.e., when all possible portion of the heat and cold loads would be provided by the heat pumps). The fact that this k value is not 100% follows directly from cost minimization considerations. Sizing the heat pumps in such a way that it would be used at full capacity only one hour per year is not cost-effective and

therefore, the optimal capacity is found to be smaller than the theoretical limit, resulting in heat pump electricity consumption profiles with a plateau as in Fig. 6.

Considering Fig. 5, it is possible to derive a direct mathematical relation for the optimal heat pump capacity, i.e. for the optimal *k* value. If the size of the heat pump is increased by a small increment *dQ*, the total cost will be changed by *dC* as

$$dC \approx \phi_{HP}\, dQ + \frac{(1+i)^n - 1}{i(1+i)^n}\left(\phi_{e,tot}\int dP_{e,HP}dt - \phi_{e,tot}\int dP_{e,\mathrm{CH}}dt - \phi_{e,tot}\int dP_{e,\mathrm{EH}}dt - \phi_f \int dP_{f,\mathrm{B}}dt\right) \quad (27)$$

where the right-hand side terms denote respectively cost variations for the heat pump purchase, heat pump consumption, chiller consumption, electric heater consumption cost, and fuel consumption due to the change of the heat pump capacity. As introduced before, the present value of the operation costs is used with the proper interest rate and number of years. The coefficient $\phi_{e,tot}$ represent the total electricity cost coefficients. The value of these coefficients have been previously given (ϕ_{HP} = 230 CAD/kW, $\phi_{e,tot}$ = 0.05057 CAD/kWh, and ϕ_f = 0.15 CAD/m^3). Note that $\phi_{e,tot}$ is the total electricity cost coefficients resulted by the summation of the rates of electricity consumption (energy) and electricity peak (maximum power). Introducing the efficiencies, it can be shown that Eq. (27) can be expressed as:

$$dC \approx \phi_{HP}\, dQ + \left(\int dP_{e,HP}dt\right)\underbrace{\left(\frac{(1+i)^n - 1}{i(1+i)^n}\right)\left[\phi_{e,tot} - \phi_{e,tot}\frac{\eta_{eh}^{HP}-1}{\eta_{ec}^{CH}} - \phi_{e,tot}\frac{\eta_{eh}^{HP}}{\eta_{eh}^{EH}} - \phi_f\frac{\eta_{eh}^{HP}}{\eta_{fh}^{B}}\right]}_{c_4} \quad (28)$$

and the minimal cost is achieved when $dC = 0$. The order of magnitude of the term $\left(\int dP_{e,HP}dt\right)$ can be estimated by evaluating the area of the two shaded areas Fig. 5, i.e. $2dQ(t_2 - t_1)/(\eta_{eh}^{HP} - 1)$. The time t_1 is found by intersecting $Q_{HP,max}/(\eta_{eh}^{HP} - 1)$ and the cooling load curve $L_c(t)/(\eta_{eh}^{HP} - 1)$. Similarly, the time t_2 is obtained by intersecting $Q_{HP,max}/(\eta_{eh}^{HP} - 1)$ by $L_h(t)/\eta_{eh}^{HP}$. One obtains:

$$\left(\int P_{e,HP}dt\right) \approx 4\frac{dQ}{(\eta_{eh}^{HP} - 1)}\frac{\tau_y}{2\pi}\left\{\mathrm{Arc}\cos\left(\frac{2\eta_{eh}^{HP}Q_{HP,\max}}{A_h(\eta_{eh}^{HP} - 1)} - 1\right) - \mathrm{Arc}\cos\left(1 - \frac{2Q_{HP,\max}}{A_c}\right)\right\} \quad (29)$$

In order to simplify the expression, the arccos functions can be approximated by

$$Arc\cos(x) \approx -1.178\,x + 157 \quad (30)$$

as long as x is between -1 and 1, which is the case here. Introducing Eqs. (30) and (29) in Eq. (28) and isolating $Q_{HP,max}$, one finds

$$Q_{HP,\max,\mathrm{math}} \approx \frac{1+\dfrac{\pi c_1}{4(1.178)\,c_4\,\tau_y\,(\eta_{eh}^{HP}-1)}}{\dfrac{\eta_{eh}^{HP}}{A_h(\eta_{eh}^{HP}-1)}+\dfrac{1}{A_c}} = \frac{1+\dfrac{\pi c_1(\eta_{eh}^{HP}-1)}{4(1.178)\,c_4\,\tau_y}}{\dfrac{\eta_{eh}^{HP}}{A_h(\eta_{eh}^{HP}-1)}+\dfrac{1}{A_c}} \tag{31}$$

The optimal heat pump capacity that we obtained in the previous section for different load scenarios versus Eq. (31) is plotted in Fig. 8. It is found that the heat pump capacity predicted by Eq. (31) is close to the one obtained from the full optimization. It is evident from Fig. 8 that the optimal heat pump sizing is almost 80% of thermodynamics limit, no matter how much the heating and cooling load amplitudes are.

The present scale analysis helps to understand how a cost-minimal heat pump system works in practice in a combined heating and cooling network. Correlations such as Eq. (31) can be used conveniently to estimate the cost-minimal sizing of the heat pumps, without having to perform the full optimization. The correlation also reveals explicitly how each parameter of the problem can influence the best solution. As a result, even if a different context was to be considered (e.g., different cost of energy, loads, cost of pump, etc.), the relations of the present section could still be used to estimate the cost minimal sizing of the heat pump without having to perform the full optimization presented before.

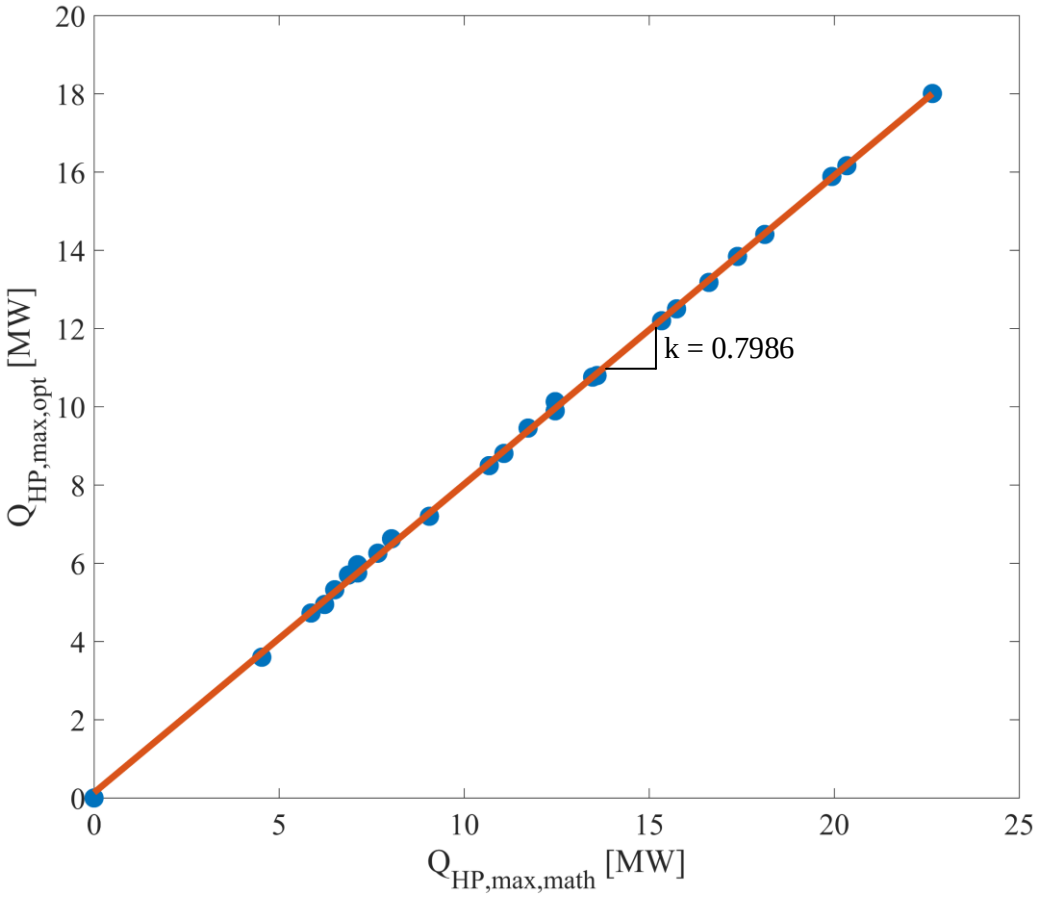

Figure 8:Optimized heat pump capacity from optimization versus thermodynamic limit based on loads

6. Dual-objective optimization

As mentioned in Section 2, in addition to minimizing the total cost of the waste heat recovery strategy, it is also often desirable to minimize the GHG emissions of the project. So far, the results presented above only considered the minimization of total cost, not CO_2 emissions. A special attention was devoted to cost minimal solutions since this is often the most widely used criterion for sizing and operating heating and cooling systems. However, since more and more emphasis is put on reducing our environmental footprint, it becomes more and more relevant to include a second objective in the problem, namely the reduction of GHG emissions. Thefore, the present section introduces a dual-objective minimization of both cost and GHG emissions, based on the weighted average sum method. Although this method does not necessarily lead exactly to the Pareto front, it is still employed often in literature. In principle, every Pareto optimal solution can be found with this method, if convexity holds [11] (which is the case here since the problem has been linearized).

The weighted average sum method minimizes a combination of the different normalized objective functions. A normalization of the objectives introduced in Section 2 is recommended in order to obtain values of the two objectives having the same order of magnitude, as this will facilitate the creation of the Pareto front. In the present case, the dual-objective optimization problem can thus be formulated as:

$$\min\left(w\tilde{C}_{tot}+(1-w)\tilde{CO}_{2,tot}\right) \tag{32}$$

where w is the weight given to the first objective function and the symbol ~ is to remind us that these functions have been normalized. The same set of constraints as before apply. To normalize the cost and emission functions, so that they can be added together, the following method can be used [11]

$$\tilde{C}_{tot}=\frac{C_{tot}-C_{\min}}{C_{\max}-C_{\min}} \tag{33}$$

$$\tilde{CO}_{2,tot}=\frac{CO_{2,tot}-CO_{2,\min}}{CO_{2,\max}-CO_{2,\min}} \tag{34}$$

The parameters C_{min}, C_{max} represent respectively, the minimum and the maximum costs of the plant when the cost is considered as the only objective function of the optimization, with minimization and maximization objectives. Similarly, $CO_{2,min}$, and $CO_{2,max}$ stand for the minimum and the maximum GHG emission while the optimization takes emission into account as the sole objective function. These values are thus unique for a pair of load amplitudes. The value of w must be between 0 and 1. By performing the optimization for different values of w, it is thus possible to build the equivalent of a Pareto front of non-dominated solutions.

The result of the dual-objective optimization is shown in Fig. 9. The minimized cost $\tilde{C}_{tot,\min}$ and minimized emissions $\tilde{CO}_{2,tot,\min}$ are shown for 9 different combinations of the heating and cooling loads. Each point is the result of optimization for a given value of w. For each load combination, 50 values of w were considered in order to plot Fig. 9. As could be expected, in order to reduce GHG emissions, it is required to increase the total cost and vice versa, to reduce the cost involves increasing GHG emissions. In the context that is simulated, natural gas is cheaper than electricity, but its usage generates more GHG emissions. Therefore, when the emphasis is put on cost, gas is preferred over electricity to satisfy the heating load. On the other hand, when the focus is on emissions, electricity emerges as the best heating

source. It should also be noted that in all load scenarios and for all values of *w*, the heat pumps are beneficial which will be demonstrated below.

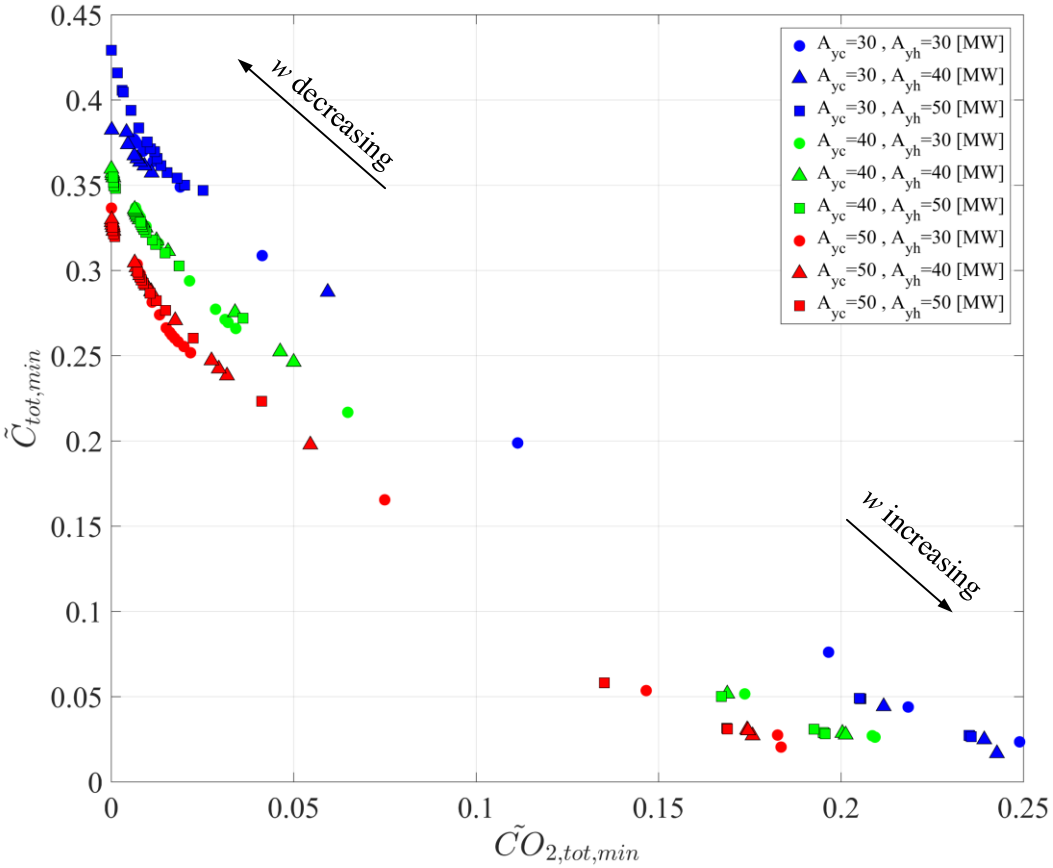

Figure 9:Pareto front associated with dual-objective optimization of cost and emission for 9 different sets of heating and cooling loads

In order to better understand how the weight given to cost versus emissions affects the optimal solution, the features of the optimal solutions reported on the Pareto front of Fig. 9 have been analyzed. In Fig. 10, the optimized heat pump capacity is plotted for the nine load scenarios as a function of the weight value *w*. The case with $w = 1$ corresponds to the minimization of cost only, and the case with $w = 0$, the minimization of CO_2 emissions only. As explained in the previous sections, the heat pump optimal sizing involves a heavy utilization of the heat pumps and is strongly affected by the load values. However, the heat pump sizing is essentially unaffected by *w*, as observable in Fig. 10.

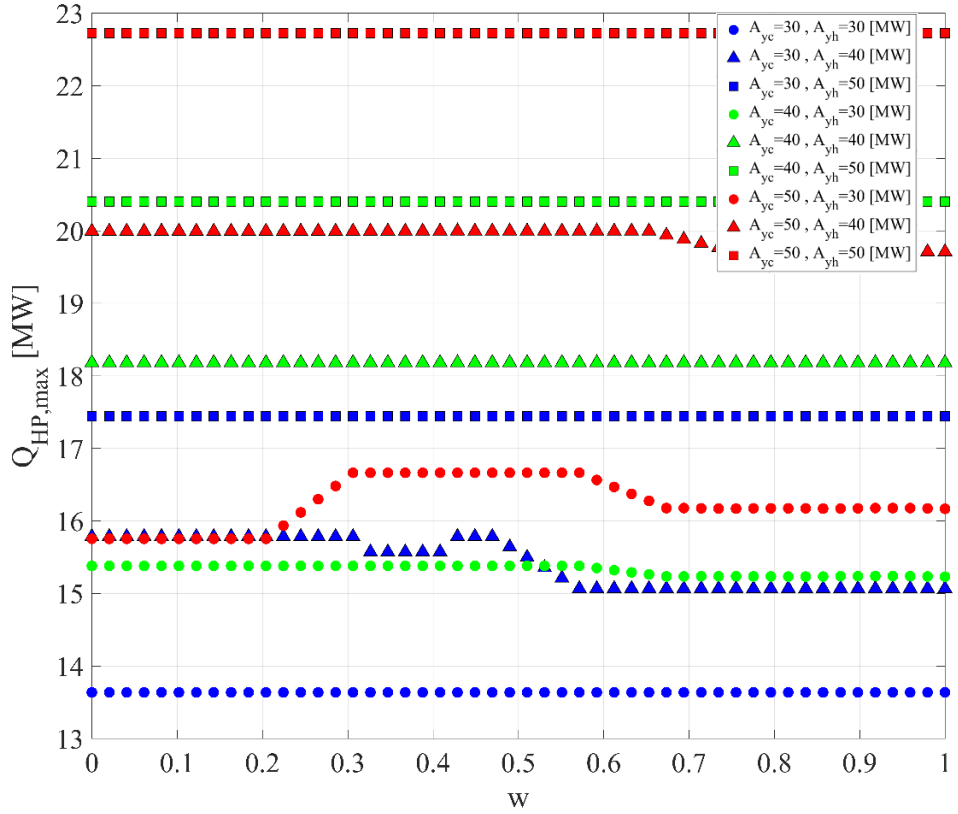

Figure 10: Optimized heat pump capacity as a function of the weight value *w* for nine load scenarios.

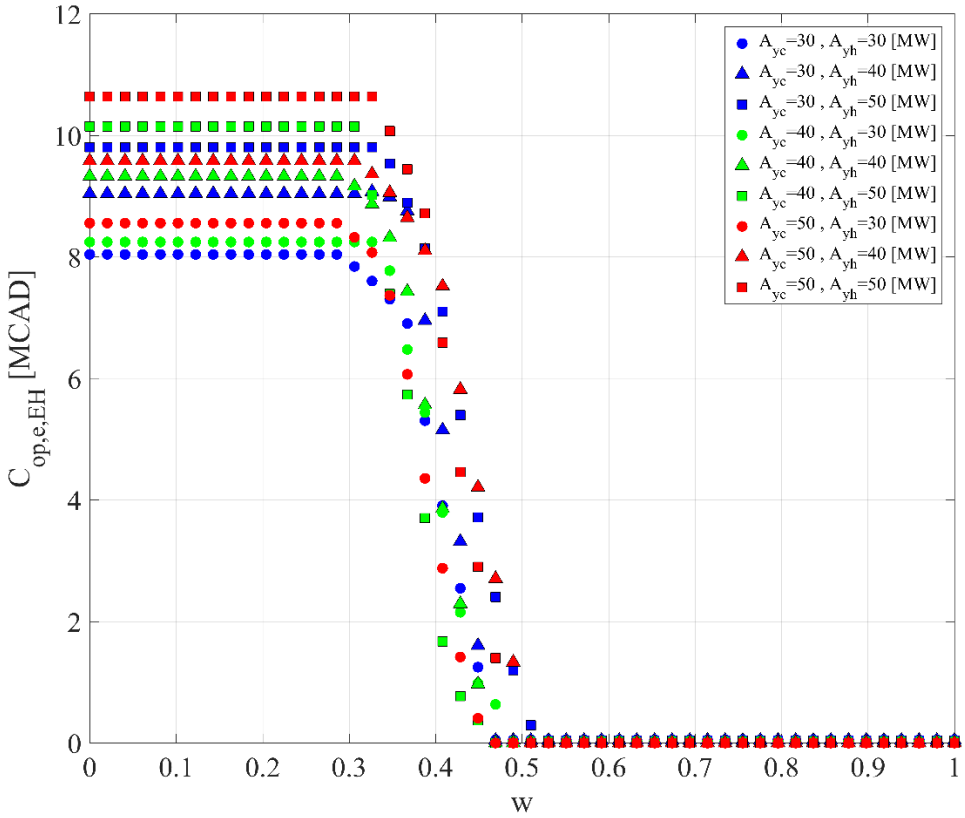

Figure 11: Electricity cost for electric heating as a function of the weight value *w* for nine load scenarios.

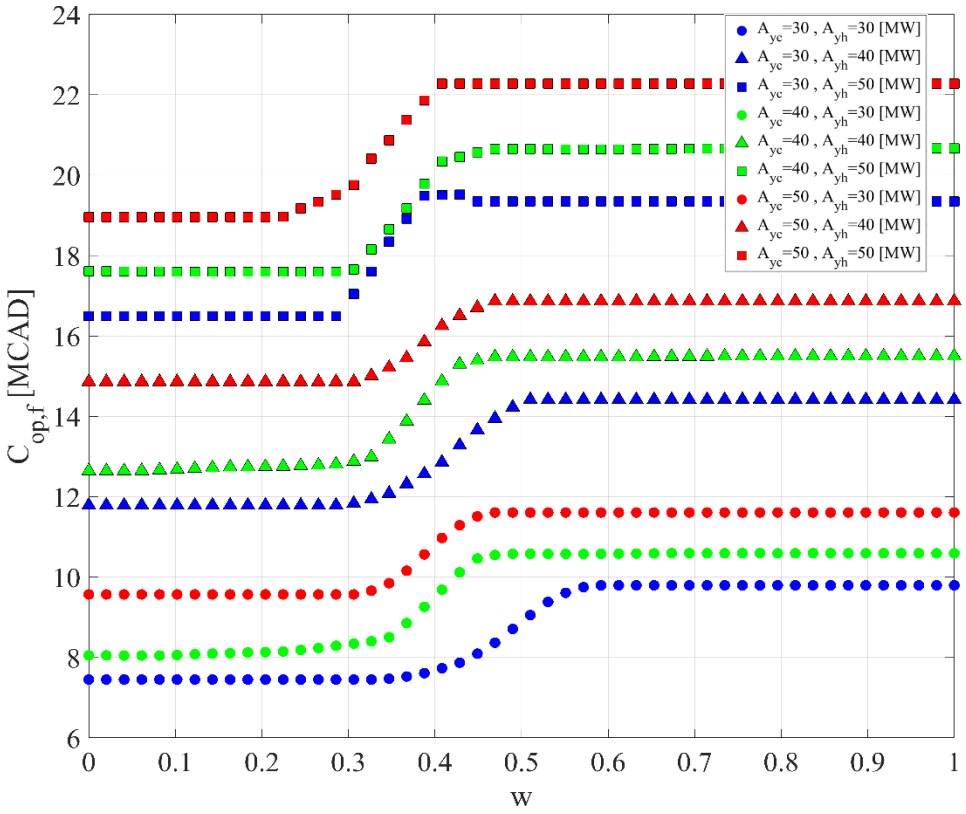

Figure 12: Cost for natural gas consumption as a function of the weight *w* for nine load scenarios.

Figure 11 presents the consumption of electricity of the electric heating system as a function of *w* and of the load scenario. It can be observed that for large *w*-values (i.e., more importance given to the cost), the electric heater is not used. This results from the fact that natural gas is cheaper, and would be preferred in that case. In Fig. 12, the consumption of natural gas is plotted and demonstrates that statement. The sharp transition around $w \sim 0.4$ corresponds to the point when electricity becomes a bon compared to gas in the overall objective function. The optimal operation strategy completely changes around that *w*-value, which explains why there is an empty space in the middle of the Pareto fronts of Fig. 9. For large *w*-values (i.e. $w > 0.4$), natural gas is used for heating providing a low cost with large emissions, whereas for small *w*-values (i.e. $w < 0.4$), electricity is preferred for heating to reduce the emissions, but at a higher cost. In other words, as *w* increases, there is at a specific *w* value a change in the optimal heating system which results in a "quantum" leap in terms of the objective function values (i.e. although the sum in Eq. (32) might not change at that *w* value, the repartition between cost and emissions does) and thus, creates a zone that is "unachievable" on the Pareto front. Note that due to the limited capacity of the electrical boiler, natural gas is still needed even when the emphasis is put on reducing GHG emissions (i.e. at low *w*-values).

The optimal use of equipment is illustrated via the Sankey diagrams of Fig. 13 for the case with $A_{h,y} = A_{c,y} = 50$ MW. In this figure, the yearly energy consumption (in MWh) of each hub technology is shown for three different values of w *(i.e.,* $w = 0$, 0.37, and 1). As apparent, the yearly energy consumption of chiller and heat pump does not change significantly with w, and it is in accordance with what is expected according to Fig. 10. The main changes is how the electric heater and the natural gas boiler are used. The conclusion was found to be similar for the other load scenarios.

It is worth to mention that the benefits of heat pumps and their sizing for simultaneous heating and cooling described above is coherent with previous studies [36]. For example, based on simulations and interviews, Kontu, Rinne and Junnila [37] showed recently that the share of heat pumps in heating networks could be increased to reduce fossil fuel consumption. The viable amount of heat pump based on heat production was estimated between 10 and 25% in the Finland context. Simultaneous cooling and heating was not considered, but they mention that heat pumps would be even more beneficial in this case. Byrne, Miriel and Lénat [38] sized a heat pump system for simultaneous heating and cooling of a large building to 80% of the heating load, but this number was not optimized. Based on Fig. 9, the optimal ratio between the heat pump capacity and the maximal heating load ranges between 35 and 50% in the present case. Averfalk, Ingvarsson, Persson, Gong and Werner [39] indicated that recently "the installations of large heat pumps [in Sweden] created an important synergy for the introduction of district cooling" but these cases were not reviewed in their study. Four district heating systems relying 100% on the district cooling network as a source of heat were reported [40]. In a case study in Sweden, Brange, Euglund and Lauenburg [41] found that exploiting the excess heat with heat pumps could cover between 50 and 120% of the annual heat demand. As can be seen, the results depicted in Figures 9-12 and in previous sections are thus consistent with test cases from literature and help to develop a better understanding of the potential synergy between heating and cooling networks. The approach proposed in this work is capable of estimating the benefits of a waste heat recovery strategy, size its components and operate it optimally.

7. Conclusions

Cooling and heating networks are among the most widely used energy systems. Thermally integrating them with heat pump is a practical way to improve their energy efficiency. The

challenge to properly design such a system for it to be economically viable and yield as much GHG emission reduction as possible is quite complex and there is a lack of tools to do so in practice. In this work, we introduced an energy hub model to optimize the design and operation of a synergetic cooling and heating network. The system includes a chiller, an electric boiler, a natural gas boiler and heat pumps. Specifically, we focused on the waste heat recovery provided by the heat pumps. Every hour of the year is considered in order to optimize how much each piece of equipment is used and to size the heat pumps for different load scenarios. The objective functions that are considered are the total cost and the CO_2 emissions.

The contributions of this investigation can be briefly summarized as follows:

-The energy hub concept was successfully adapted for the optimization of waste heat recovery in cooling and heating networks with heat pumps. We were able to achieve a linear model that solved relatively fast and that could provide a significant insight on the optimal features of the system;

-In the different scenarios investigated, the use of heat pumps to recover heat from the cooling loop always proved to be beneficial in terms of both cost and emissions. The heat pump optimal capacity is around 80% of the thermodynamic maximal value based on the load analysis.

-A theoretical analysis of the system was performed and was able to provide the correct order of magnitude for the optimal sizing of the heat pump. By comparing the analysis to the formal optimization results, we obtained correlations that can be used to easily size the heat pump system.

-The weighted sum average method allowed generating a Pareto front when minimizing simultaneously cost and GHG emissions. A relatively sharp transition between two families of solutions was noted at the point when electricity becomes more viable an option than gas for heating in the combined objective function as more emphasis is put on CO_2 than on cost.

The results were shown to be in line with current literature and help to fill the lack of knowledge on optimized synergetic heating and cooling networks. The figures and correlations that have been developed in this work can serve as straightforward design tools for practice engineers to properly size and operate such systems.

Future work could include a better representation of system. For example, the efficiencies could vary with part-load factors and outside temperature. The integration of other potential technologies such as energy storage and renewables (PV, geothermal, etc.) could be

optimized. Finally, it would be interesting to perform a sensitivity analysis of uncertain parameters or parameters that could change over time (e.g., costs, loads, etc.).

Acknowledgments

This work was supported by the Natural Sciences and Engineering Research Council of Canada (NSERC).

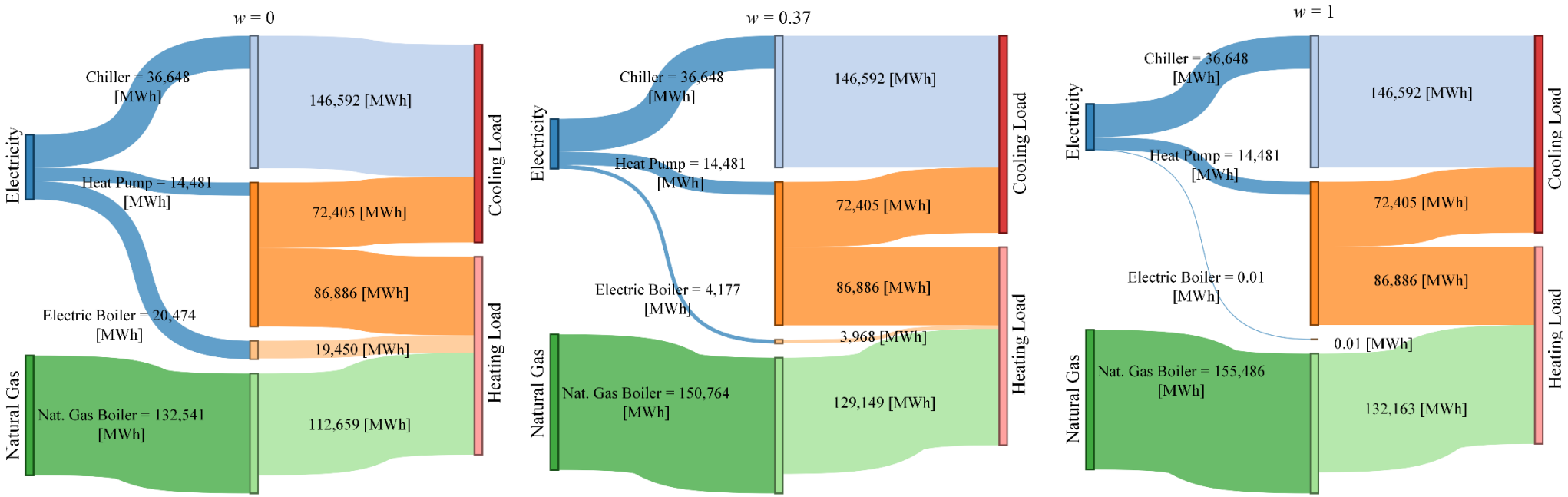

Figure 13: Sankey diagram of energy use for $A_{h,y} = A_{c,y} = 50$ MW and for three weights (w = 0, 0.37 and 1).

References

[1] P. Favre-Perrod, “A vision of future energy networks,” in *2005 IEEE Power Engineering Society Inaugural Conference and Exposition in Africa*, 2005, pp. 13–17.

[2] M. Geidl, G. Koeppel, P. Favre-Perrod, B. Klockl, G. Andersson, and K. Frohlich, “Energy hubs for the future,” *IEEE Power Energy Mag.*, vol. 5, no. 1, pp. 24–30, 2007.

[3] M. Geidl, Gaudenz Koeppel, Patrick Favre-Perrod, Bernd Klöckl, Göran Andersson, and Klaus Fröhlich, “The Energy Hub – A Powerful Concept for Future Energy Systems,” presented at the Annual Carnegie Mellon Conference on the Electricity Industry, ETH Zurich, Switzerland, 2007.

[4] M. Geidl, “Integrated modeling and optimization of multi-carrier energy systems,” 2007.

[5] M. Geidl and G. Andersson, “A modeling and optimization approach for multiple energy carrier power flow,” in *2005 IEEE Russia Power Tech*, 2005, pp. 1–7.

[6] M. Geidl and G. Andersson, “Optimal power dispatch and conversion in systems with multiple energy carriers,” in *Proc. 15th Power Systems Computation Conference (PSCC)*, 2005.

[7] M. Geidl and G. Andersson, “Operational and structural optimization of multi-carrier energy systems,” *Eur. Trans. Electr. Power*, vol. 16, no. 5, pp. 463–477, 2006.

[8] M. Geidl and G. Andersson, “Optimal Power Flow of Multiple Energy Carriers,” *IEEE Trans. Power Syst.*, vol. 22, no. 1, pp. 145–155, Feb. 2007.

[9] M. Schulze, L. Friedrich, and M. Gautschi, “Modeling and optimization of renewables: applying the Energy Hub approach,” in *2008 IEEE International Conference on Sustainable Energy Technologies*, 2008, pp. 83–88.

[10] A. Maroufmashat, A. Elkamel, M. Fowler, S. Sattari, R. Rochandel, A. Hajimiragha, S. Walker, E. Entchev, “Modeling and optimization of a network of energy hubs to improve economic and emission considerations,” *Energy*, vol. 93, pp. 2546–2558, 2015.

[11] O. Grodzevich and O. Romanko, “Normalization and other topics in multi-objective optimization,” in *Proceedings of the Fields-MITACS Industrial Problems Workshop*, 2006.

[12] I. G. Moghaddam, M. Saniei, and E. Mashhour, “A comprehensive model for self-scheduling an energy hub to supply cooling, heating and electrical demands of a building,” *Energy*, vol. 94, pp. 157–170, 2016.

[13] Y. Wang, N. Zhang, Z. Zhuo, C. Kang, and D. Kirschen, “Mixed-integer linear programming-based optimal configuration planning for energy hub: Starting from scratch,” *Appl. Energy*, vol. 210, pp. 1141–1150, Jan. 2018.

[14] B. Guler, E. Çelebi, and J. Nathwani, “A ‘Regional Energy Hub’ for achieving a low-carbon energy transition,” *Energy Policy*, vol. 113, pp. 376–385, Feb. 2018.

[15] G. T. Ayele, P. Haurant, B. Laumert, and B. Lacarrière, “An extended energy hub approach for load flow analysis of highly coupled district energy networks: Illustration with electricity and heating,” *Appl. Energy*, vol. 212, pp. 850–867, Feb. 2018.

[16] A. Maroufmashat, M. Fowler, S. Sattari Khavas, A. Elkamel, R. Roshandel, and A. Hajimiragha, “Mixed integer linear programing based approach for optimal planning and

operation of a smart urban energy network to support the hydrogen economy," *Int. J. Hydrog. Energy*, vol. 41, no. 19, pp. 7700–7716, May 2016.

[17] A. Sharif, A. Almansoori, M. Fowler, A. Elkamel, and K. Alrafea, "Design of an energy hub based on natural gas and renewable energy sources," *Int. J. Energy Res.*, vol. 38, Mar. 2014.

[18] K. AlRafea, M. Fowler, A. Elkamel, and A. Hajimiragha, "Integration of renewable energy sources into combined cycle power plants through electrolysis generated hydrogen in a new designed energy hub," *Int. J. Hydrog. Energy*, vol. 41, no. 38, pp. 16718–16728, Oct. 2016.

[19] T. Togawa, T. Fujita, L. Dong, M. Fujii, and M. Ooba, "Feasibility assessment of the use of power plant-sourced waste heat for plant factory heating considering spatial configuration," *J. Clean. Prod.*, vol. 81, pp. 60–69, 2014.

[20] A. Shahmohammadi, M. Moradi-Dalvand, H. Ghasemi, and M. S. Ghazizadeh, "Optimal design of multicarrier energy systems considering reliability constraints," *IEEE Trans. Power Deliv.*, vol. 30, no. 2, pp. 878–886, 2015.

[21] S. Pazouki and M.-R. Haghifam, "Optimal planning and scheduling of energy hub in presence of wind, storage and demand response under uncertainty," *Int. J. Electr. Power Energy Syst.*, vol. 80, pp. 219–239, 2016.

[22] F. Brahman, M. Honarmand, and S. Jadid, "Optimal electrical and thermal energy management of a residential energy hub, integrating demand response and energy storage system," *Energy Build.*, vol. 90, no. Supplement C, pp. 65–75, Mar. 2015.

[23] M. Batić, N. Tomašević, G. Beccuti, T. Demiray, and S. Vraneš, "Combined energy hub optimisation and demand side management for buildings," *Energy Build.*, vol. 127, pp. 229–241, 2016.

[24] F. Kamyab and S. Bahrami, "Efficient operation of energy hubs in time-of-use and dynamic pricing electricity markets," *Energy*, vol. 106, pp. 343–355, 2016.

[25] M. Mohammadi, Y. Noorollahi, B. Mohammadi-ivatloo, and H. Yousefi, "Energy hub: From a model to a concept – A review," *Renew. Sustain. Energy Rev.*, vol. 80, pp. 1512–1527, Dec. 2017.

[26] S. Moradi, R. Ghaffarpour, A. M. Ranjbar, and B. Mozaffari, "Optimal integrated sizing and planning of hubs with midsize/large CHP units considering reliability of supply," *Energy Convers. Manag.*, vol. 148, pp. 974–992, Sep. 2017.

[27] A. Sheikhi, A. M. Ranjbar, H. Oraee, and A. Moshari, "Optimal operation and size for an energy hub with CCHP," *Energy Power Eng.*, vol. 3, no. 05, p. 641, 2011.

[28] A. Sheikhi, A. M. Ranjbar, and H. Oraee, "Financial analysis and optimal size and operation for a multicarrier energy system," *Energy Build.*, vol. 48, no. Supplement C, pp. 71–78, May 2012.

[29] R. Croteau and L. Gosselin, "Correlations for cost of ground-source heat pumps and for the effect of temperature on their performance," *Int. J. Energy Res.*, vol. 39, no. 3, pp. 433–438, Mar. 2015.

[30] D. Setlhaolo, S. Sichilalu, and J. Zhang, "Residential load management in an energy hub with heat pump water heater," *Appl. Energy*, vol. 208, pp. 551–560, Dec. 2017.

[31] "https://www.energir.com/en/business/price/natural-gas-price/."

[32] “Rate L - Business.” [Online]. Available: http://www.hydroquebec.com/business/customer-space/rates/rate-l-industrial-rate-large-power-customers.html. [Accessed: 26-Oct-2018].

[33] “GHG emissions and electricity | Hydro-Québec.” [Online]. Available: http://www.hydroquebec.com/developpement-durable/centre-documentation/taux-emission-ges.html. [Accessed: 14-Feb-2018].

[34] “Mandatory reporting of certain emissions of contaminants into the atmosphere; draft regulations, Gazette N° 23 du 2010-06-09 Page : 1397.” [Online]. Available: http://www2.publicationsduquebec.gouv.qc.ca/dynamicSearch/telecharge.php?type=1&file=2010A%2F9832.PDF. [Accessed: 26-Oct-2018].

[35] H. P. Williams, *Model Building in Mathematical Programming*. John Wiley & Sons, 2013.

[36] P. Byrne, J. Miriel, and Y. Lenat, “Experimental study of an air-source heat pump for simultaneous heating and cooling–part 1: basic concepts and performance verification,” *Appl. Energy*, vol. 88, no. 5, pp. 1841–1847, 2011.

[37] K. Kontu, S. Rinne, and S. Junnila, “Introducing modern heat pumps to existing district heating systems – Global lessons from viable decarbonizing of district heating in Finland,” *Energy*, vol. 166, pp. 862–870, Jan. 2019.

[38] P. Byrne, J. Miriel, and Y. Lénat, “Modelling and simulation of a heat pump for simultaneous heating and cooling,” in *Building simulation*, 2012, vol. 5, pp. 219–232.

[39] H. Averfalk, P. Ingvarsson, U. Persson, M. Gong, and S. Werner, “Large heat pumps in Swedish district heating systems,” *Renew. Sustain. Energy Rev.*, vol. 79, pp. 1275–1284, Nov. 2017.

[40] A. David, B. V. Mathiesen, H. Averfalk, S. Werner, and H. Lund, “Heat Roadmap Europe: Large-Scale Electric Heat Pumps in District Heating Systems,” *Energies*, vol. 10, no. 4, p. 578, Apr. 2017.

[41] L. Brange, J. Englund, and P. Lauenburg, “Prosumers in district heating networks – A Swedish case study,” *Appl. Energy*, vol. 164, pp. 492–500, Feb. 2016.

Figure captions

Figure 1: Hub representation of a heating and cooling network including electrical and natural gas boilers (eb and fb), chillers (ch) and heat pumps (hp).

Figure 2: Schematic representation of the heating, cooling and electricity loads.

Figure 3: Savings caused by heat pumps (cost difference between the reference hub and that cost-minimized hub with the heat pumps) as a function of the heating and cooling.

Figure 4: Optimal heat pump capacity as a function of the heating and cooling loads with constant electrical load.